Infrared transmissive, hollow plastic waveguides with inner Ag–AgI coatings

Roshan George and James A. Harrington

Hollow polycarbonate waveguides with thin-film coatings of Ag–AgI were fabricated by liquid-phase chemistry methods. These hollow waveguides, which have bore sizes ranging from 500 to 2000 μm and lengths as long as 2 m, are transmissive from 2 to more than 20 μm. The lowest loss of 0.02 dB/m was obtained for a straight 2000 μm bore guide at 10.6 μm. This is to our knowledge the lowest loss measured for any IR fiber at CO_2 laser wavelengths. The bending losses were found to increase as $1/R$, where R is the radius of the bend. These waveguides were able to withstand 18 W of CO_2 laser input power for bore sizes greater than 1000 μm. © 2005 Optical Society of America

OCIS codes: 060.2390, 160.4760, 310.6860.

1. Introduction

Hollow waveguides have been fabricated for more than 20 years for the transmission of IR wavelengths longer than 2 μm. These unusual hollow-core fiber optics comprise flexible, structurally supportive tubing made from metal, glass, or plastic, with inner reflective metallic and dielectric coatings. Although there have been many combinations of metallic and dielectric coatings deposited inside structural tubing, one of the most successful and lowest-loss hollow guides has been Ag–AgI-coated hollow glass waveguides (HGWs). The Ag–AgI HGWs have been fabricated with losses as low as 0.2 dB/m at 10.6 μm, in bore sizes ranging from 250 to 1000 μm, and in lengths as long as 13 m. Recently, Harrington reviewed the properties of hollow waveguides in general and gave a detailed treatment of some of the sensor and laser power delivery applications for this unique category of fiber optics.[1]

Hollow-core waveguides operate on somewhat different principles from solid-core fibers. In particular, there are two distinguishing characteristics of hollow guides not shared by solid-core fibers. First, the loss varies as $1/a^3$, where a is the bore radius, and second, there is an additional loss for most hollow guides on bending that is proportional to the curvature, or $1/R$, where R is the radius of the bend. The $1/R$ bending loss is the most common case, but it is possible to design a one-dimensional hollow structure that will have no bending loss. These are the so-called omnidirectional waveguides, which exhibit a photonic bandgap as a result of the deposition of alternating layers of high-contrast refractive-index films.[2,3] The $1/a^3$ bore size loss clearly implies that the easiest method to reduce the losses is merely to increase the bore size. For the waveguides made from either silica or metal (nickel or stainless-steel) tubing it is impractical to go to bore sizes greater than ~1000 μm because the tubing is essentially inflexible. To achieve lower loss and at the same time maintain good flexibility we have chosen to use polycarbonate tubing with bore sizes ranging from 500 to 2000 μm. Polycarbonate tubing is quite flexible in the bore sizes up to 6000 μm, and the inner surface roughness, although it is not quite so low as for drawn silica glass tubing, is quite small. The metallic Ag and dielectric AgI coatings are applied by use of a liquid-phase chemistry process much like that used to coat silica tubing.[4] The losses for the hollow polycarbonate waveguides (HPWs) that we have measured are lower than the lowest loss for a HGW. Specifically, the lowest loss for the 2000 μm bore HPW is approximately 0.02 dB/m at 10.6 μm.

2. Experimental Methods

A. Structure and Sensitization of Hollow Polycarbonate Waveguides

The structure of a Ag–AgI HPW made from polycarbonate tubing is shown in Fig. 1. We obtained extruded polycarbonate tubing in 2 m lengths with bore

R. George and J. A. Harrington (jaharrin@rci.rutgers.edu) are with the Department of Materials Science and Engineering, Rutgers University, Piscataway, New Jersey 08854.

Received 6 April 2005; accepted 6 April 2005.
0003-6935/05/306449-07$15.00/0

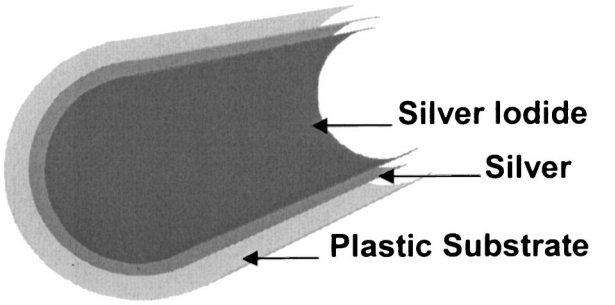

Fig. 1. Structure of the hollow polycarbonate waveguide, showing the Ag and AgI dielectric films for high reflectivity.

sizes of 500, 700, 1000, 1500, and 2000 μm from Drummond Scientific and Extrusioneering. Polycarbonate is an excellent optical polymer, which is quite strong and, therefore, resistant to distortion on bending, and it has a maximum service temperature of 130 °C. All the HPWs fabricated in the study reported here were coated for optimal performance at the CO_2 laser wavelength of 10.6 μm. An initial account of this study has been given by Haan and Harrington.[5]

Polymer tubing requires the use of a sensitizer before the deposition of the metallic coating. The palladium-stannous-based sensitizer that we used reduces the surface energy of the polymer by forming a seed layer, which promotes adhesion of the film to the plastic. The palladium-based catalyst consists of a mixture of palladium and tin salts dissolved in an acidic solution.[6] Specifically, we prepared a 100 ml sensitizing solution, using 0.05 g of $PdCl_2$ and 2.5 g of $SnCl_2$ dissolved in 100 ml of dilute hydrochloric acid with a pH of 1.0. First the polymer tube is rinsed with deionized H_2O, and then the sensitizing solution is circulated through the tubing for approximately 2–5 min. The colloidal palladium-stannous mixture is physisorbed on the walls of tube, and this is visible as a brown translucent film. This film is removed and the surface activated by rinsing with a 5% NaOH solution for ~2 min. We also used a commercial sensitizer of essentially the same composition, from Shipley Corporation, Inc. The advantage of their sensitizer is that it is more stable and lasts as long as a month.

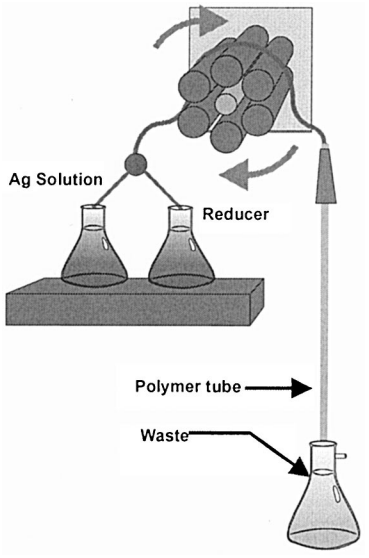

Fig. 2. Experimental arrangement for the deposition of Ag films inside polycarbonate tubing. A peristaltic pump is used to force the solutions through the tubing. A similar setup is used for iodization to form the AgI coating.

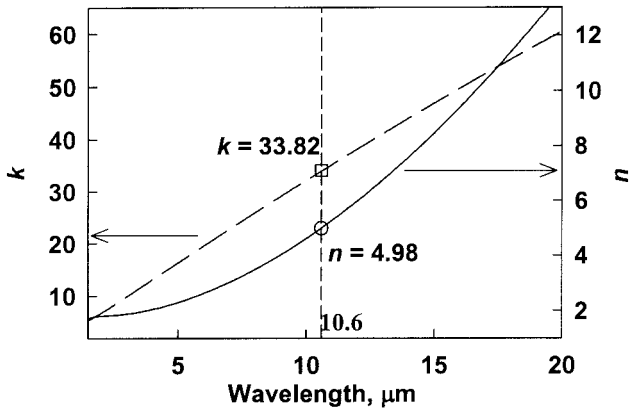

Fig. 3. Optical constants for Ag films measured with a spectroscopic ellipsometer.

B. Deposition of Ag–AgI Films

The deposition of the thin-film layers on the sensitized polymer substrate is similar to the methods used to coat the hollow glass tubing with Ag–AgI films. The coating of Ag and AgI films on glass substrates has been thoroughly studied and optimized by Rabii *et al.*[7] Dahan *et al.* used similar techniques with slightly different precursors to fabricate the thin films for their polymer waveguides.[8]

The first step in the process is silvering the sensitized polycarbonate tubing. This is done with a Ag solution and a reducer solution, as shown in Fig. 2. We prepare the Ag solution by dissolving 2.4 g of $AgNO_3$ in 800 ml of pure H_2O and then adding a mixture of 6% NH_4OH and

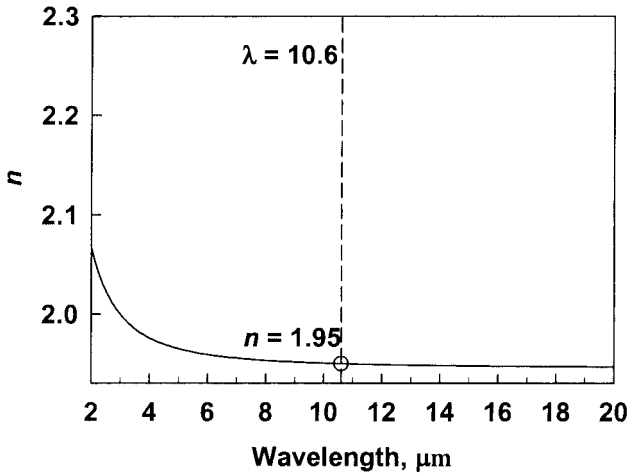

Fig. 4. Refractive index for a AgI film deposited on to a Ag film. Measurements were made with a spectroscopic ellipsometer.

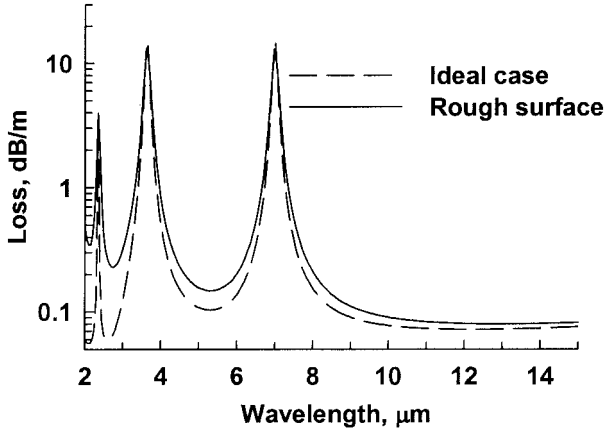

Fig. 5. Calculated spectral loss for a 1000 μm bore Ag–AgI waveguide. The ideal case assumes perfectly smooth films and substrate, whereas the rough surface calculations were made with our measured values for the surface roughness of Ag and AgI films.

0.44 g NaOH to complex the silver and improve the adhesion, durability, and hardness of the Ag layer.[9] We prepare the reducer solution by dissolving 0.08 g of sodium ethylene-diamine tetraacetic acid (Na_2EDTA) and 0.56 g of dextrose in pure H_2O. A thin Ag film is deposited at a rate of ~1 μm/h when the two solutions are mixed and pumped through the tubing at a flow rate of 5–10 ml/min by a peristaltic pump, as shown in Fig. 2.

The AgI dielectric layer is formed by a subtractive process in which an iodine solution reacts with the Ag layer and converts part of the Ag film to AgI. In forming the AgI layer from the Ag film it is important that the Ag layer be sufficiently thick that an adequate reflective layer of Ag remain under the AgI layer. That is, the Ag film should be much greater than the skin depth (10 to 30 nm in the mid-IR region); otherwise the light will penetrate through the Ag film into the silica tubing and be absorbed. Most of the Ag films that we deposited were approximately 200 nm thick.

The optimal thickness of the single-layer AgI film for transmission of the lowest-loss HE_{11} mode for a given wavelength is given by

$$\delta a_{\mathrm{AgI}} = \frac{\lambda_0}{2\pi\sqrt{n_{\mathrm{AgI}}^2 - 1}} \tan^{-1}\left[\frac{n_{\mathrm{AgI}}}{(n_{\mathrm{AgI}}^2 - 1)^{1/4}}\right], \qquad (1)$$

where n_{AgI} is the refractive index of AgI at 10.6 μm. We measured the refractive index of AgI, using an IR ellipsometer, and found that n_{AgI} is 1.95 at 10.6 μm. Using Eq. (1), we found that the optimum thickness of the AgI layer at 10.6 μm is $\delta a_{\mathrm{AgI}} = 0.995$ μm. Hence the thickness of the deposited Ag layer should be at least 1.2 μm. This thickness of Ag is deposited in approximately 70 min.

We form the AgI film on the Ag layer by flowing a solution containing iodine dissolved in cyclohexane over the Ag film, using a setup similar to that shown in Fig. 2. The growth of the dielectric layer follows the usual kinetic reaction, $\delta a_{\mathrm{AgI}} = (Kt)^{1/m}$, where t is the

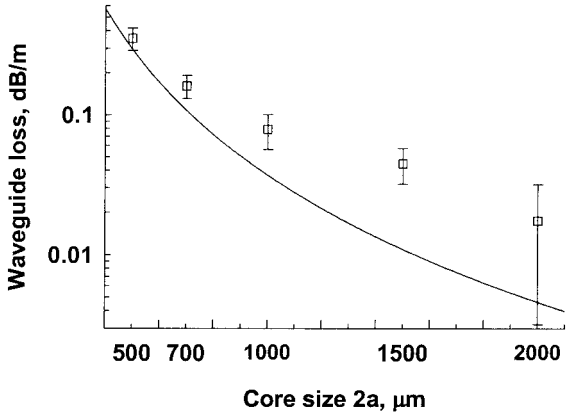

Fig. 6. Measured (open squares) loss at 10.6 μm for several bore sizes of waveguides. The calculated (solid curve) values are for the HE_{11} mode.

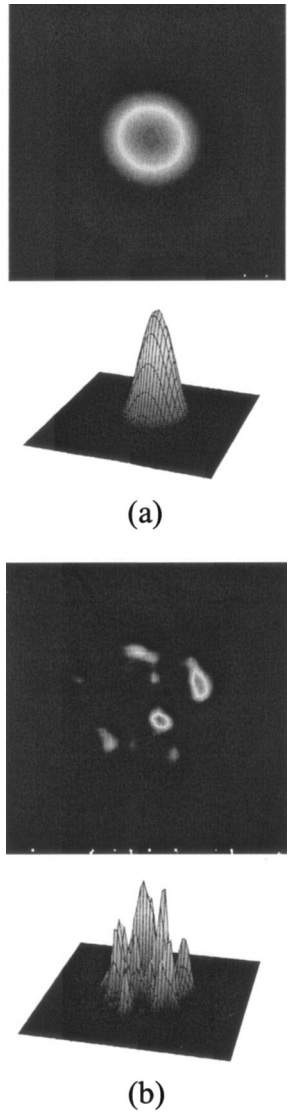

Fig. 7. Spatial output mode profiles of (a) 500 and (b) 2000 μm bore hollow polycarbonate waveguide with a TEM_{00} input from a CO_2 laser.

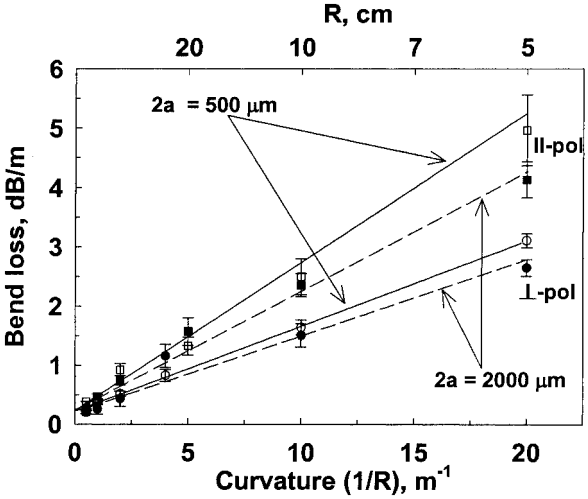

Fig. 8. Bending losses for 500 and 2000 μm bore waveguides for bending in planes parallel and perpendicular to the plane of bending.

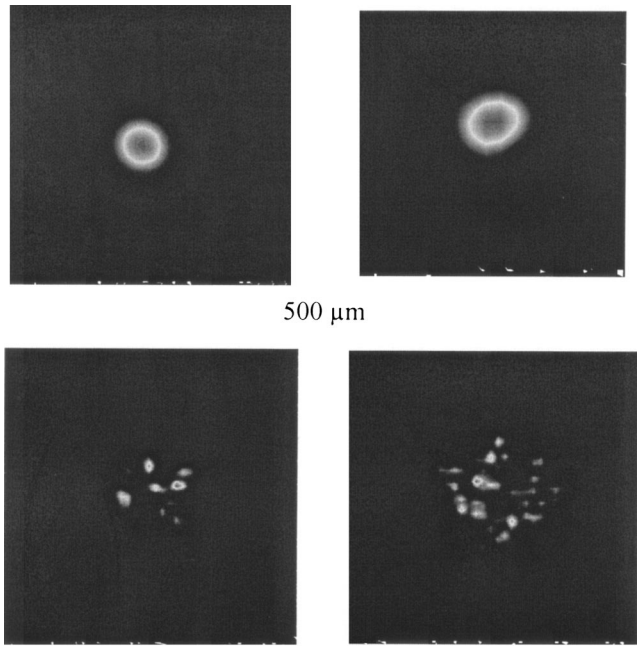

Fig. 9. Spatial output mode profile for straight (left) and bent (right, $R = 0.1$ m) 500 and 2000 μm bore waveguides.

iodination reaction time; m is a constant equal to 2.8,[10] and K is the reaction constant that depends on the iodine concentrations. To achieve the targeted AgI film thickness of approximately 1 μm, the iodination reaction is carried out at a flow rate of 15 ml/min for 180 s. Using Eq. (1) and the spectral data for a 1.5 m long waveguide, we determined the end-to-end thickness variation of the AgI film. We found that the thickness variation is less than 1%/m for our AgI thin films.

3. Experimental Results

A. Optical Constants of Ag and AgI Thin Films

The optical constants of the bulk material can be quite different from those of the thin films. To thoroughly characterize and model the optical properties of the Ag–AgI waveguide we require accurate values of the optical constants of the guiding layers. The values of the film's optical constants, n and k, were measured with a Sopra spectroscopic ellipsometer. This ellipsometer is capable of measuring n and k from 0.19 to 17 μm. The only input parameter was film thickness, and this was measured with either a field emission scanning-electron microscope or a profilometer. Thin films for ellipsometry were deposited on to glass slides by the same methods used to deposit the films in the waveguides.

The 200 μm thickness of the Ag thin films was greater than the skin depth, so the values that we obtained for n and k are close to those published.[11] Our data for constants n and k for Ag are given in Fig. 3. A regression analysis was performed on the data in Fig. 3 to produce curve fits for n (goodness of fit, $R^2 = 99.99\%$) and k ($R^2 = 99.96\%$). The resultant equations for the optical constants of Ag are

$$n(\lambda) = 1.8454 - 0.1186\lambda + 0.0443\lambda^2 - 0.0005\lambda^3,$$

$$k(\lambda) = 119.97 - \frac{1720}{\lambda} + \frac{11677.07}{\lambda^2} - \frac{37261.57}{\lambda^3} + \frac{44833.36}{\lambda^4}, \quad (2)$$

where λ is in micrometers.

The AgI layer is transparent through the entire IR range of the ellipsometer, so the light is reflected back from the Ag–AgI interface. Hence, for proper analysis of the optical properties of the AgI film, the multiple reflection paths from the top (AgI–air interface) and bottom (AgI–Ag interface) surfaces of the dielectric layer have to be taken into consideration. Figure 4 gives the values of n extracted for the AgI film. As expected, n has a slightly higher value in the 2–3 μm region than at 10.6 μm. At longer wavelengths, n falls to ~1.95 and remains reasonably constant at the longer IR wavelengths. A regression analysis (goodness of fit, $R^2 = 99.89\%$) was performed on the index data in the range 1–20 μm, with the resultant Cauchy relation being given by

$$n(\lambda) = 1.956 - \frac{0.239}{\lambda} + \frac{1.920}{\lambda^2} - \frac{2.678}{\lambda^3} + \frac{1.233}{\lambda^4}, \quad (3)$$

where λ is in micrometers.

Measured extinction coefficient k, over the entire mid-IR region (λ = 2–20 μm), was below the mea-

surement limits of the instrument ($k \sim 10^{-3}$). We calculated the effect on waveguide loss at 10.6 μm for k ranging from 10^{-5} to 10^{-1} and found that the loss is practically insensitive to changes in extinction coefficient when k is below 10^{-3}. Specifically, for an AgI layer with $k = 10^{-3}$, the transmission loss increases by ~2.4%/m over a lossless dielectric. Hence the AgI film has almost ideal properties in the mid IR, as the losses for the AgI films of thickness less than 1 μm are extremely small. At the all-important CO_2 laser wavelength, the measured optical constants for the AgI layer are $n = 1.95$ and $k < 10^{-3}$, which may be compared to the published value of $n = 2.1$.[11] The reason for the lower value is that our measurements were preformed on thin films, whose values can be lower than the value of bulk material.

B. Effect of the Surface Roughness of Ag and AgI Thin Films on Loss

The reflectivity of the waveguide walls is altered significantly by the roughness of the thin-film coatings. We measured the surface roughness of the substrate tube and the thin-film layers by using an atomic-force microscope and then used these roughness results to calculate the increase in loss expected for the rough films over perfectly smooth films. The rms surface roughness of the polycarbonate tubing was $\sigma_{rms} = 0.7$ nm; in contrast, silica tubing has a rms surface roughness of $\sim\sigma_{rms} = 0.2$ nm. The roughness of the Ag and AgI films depends on the thickness of the films, which in turn depends on the deposition time. Because this is a diffusion-controlled process, we would expect that $\sigma = At^p$. From our data on surface roughness and deposition time for the Ag films, we found $A = 5.88$ and $p = 0.45$ ($R^2 = 98.63\%$), values that are close to the $t^{1/2}$ dependence obtained by Rabii *et al.*[7] for Ag-coated silica HGWs. The surface roughness of a 1 μm thick AgI film (optimal thickness for 10.6 μm operation) was measured to be $\sigma_{rms} = 55$ nm when the film was deposited on to a 200 nm thick Ag layer on the polycarbonate substrate.

We used the standard equation[12] that describes the reflectivity of a rough interface between two media [the i and $(i + 1)$ layers]:

$$r_{i+1} = r_{i+1,i} A_{i+1,i} + \frac{(1 - r_{i+1,i}^2) B_{i+1,i}^2 r_i \exp(-jk_i)}{1 + r_{i+1,i} A_{i+1,i} r_i \exp(-jk_i)}, \quad (4)$$

where

$$A_{i+1,i} = \exp\left[-\frac{1}{2}(2k_0\sigma_{i+1,i} n_{i+1} \sin\theta_{i+1})^2\right],$$

$$B_{i+1,i} = \exp\left\{-\frac{1}{2}[k_0\sigma_{i+1,i}(n_{i+1}\sin\theta_{i+1} - n_i \sin\theta_i)]^2\right\}.$$

We used the measured surface roughness of the Ag and AgI layers to calculate the waveguide loss with roughness. These results were then compared with the loss for ideal, perfectly smooth waveguides. The waveguide loss was computed from[13]

$$2\alpha = \frac{1 - R}{2a \cot\theta}. \quad (5)$$

Specifically, we considered a waveguide operating at 10.6 μm with a 200 nm Ag film over which is deposited a 1 μm thick AgI film. The roughness of these 1.2 μm thick Ag–AgI films was 20 nm at the Ag–AgI interface and 55 nm at the surface of the AgI–air interface. Using Eq. (4), we calculated the reflectivity of each rough interface and then computed the absorption, using Eq. (5). The calculated transmissions for a 1000 μm bore waveguide are shown in Fig. 5. As may be seen from the spectral data in Fig. 5, the losses for the perfectly smooth waveguide ($\sigma_{rms} = 0$) are lower than that for a waveguide with rough walls. The difference in loss is greatest at the shorter wavelengths as a result of increasing scattering. At 10.6 μm, the loss with roughness is ~15% greater than in the ideal case for which the loss is 0.074 dB/m. Ben David *et al.* reported similar results in a comparison of the waveguide loss in the near-IR region with the CO_2 wavelength.[14]

C. Losses in Hollow Polycarbonate Waveguides

Loss measurements for both straight and bent waveguides were made with a stabilized CO_2 laser with a Gaussian output. We accomplished optimal coupling into the lowest-order HE_{11} mode by varying slightly the f/number launch, as suggested by Nubling and Harrington.[15] The waveguides were 2 to 2.5 m long, and 10 to 15 samples of each bore size were measured. In Fig. 6 we show the losses for the straight waveguides along with the calculated loss for the HE_{11} mode. The loss is seen to decrease with increasing bore size, but not so strongly as $1/a^3$. We note from Fig. 6 that the lowest loss is for the 2000 μm bore waveguide with a loss of 0.02 ± 0.01 dB/m. To our knowledge this is the lowest loss measured to date for a hollow waveguide at 10.6 μm.

The data in Fig. 6 show that the measured loss is greater than the loss calculated for the HE_{11} mode. This discrepancy is due largely to the propagation of higher-order modes, which have a greater loss than the lowest-order HE_{11} mode. Attenuation coefficients α_{nm} for the HE_{nm} modes are given by

$$\alpha_{nm} = \left(\frac{u_{nm}}{2\pi}\right)^2 \frac{\lambda^2}{a^3} \mathrm{Re}(v_n) = \left(\frac{u_{nm}}{2\pi}\right)^2 \frac{\lambda^2}{a^3} \mathrm{Re}\left[\frac{\frac{1}{2}(v_n^2 + 1)}{\sqrt{v_n^2 - 1}}\right], \quad (6)$$

where v_n is the complex refractive index of the wall material and u_{nm} is the usual fiber mode parameter.[16] We observed the influence of higher-order modes on the overall loss in two ways. First, we measured the divergence angle, θ_{nm}, of the output beam for the

different bore sizes. The divergence angle is given by

$$\theta_{nm} = \sin^{-1}\left(\frac{u_{n-1,m}}{2ak_0}\right), \tag{7}$$

where $u_{n-1,m}$ is the mth zero of the Bessel function of $(n-1)$st order and $2a$ and k_0 are the core size and the wave vector, respectively. For example, the average values of divergence angles measured for the 500 and 2000 μm bore waveguides were 1.31° and 1.37°, compared to the values of 0.93° and 0.25° calculated for the HE_{11} mode. From our measurements of all bore sizes, we can conclude that the 500, 700, and 1000 μm hollow plastic waveguides propagate the HE_{11} and HE_{12} modes. For the larger bore sizes of 1500 and 2000 μm, even more modes propagate, and the discrepancy between the measured and calculated losses for these large bore sizes is even greater, as may be seen from Fig. 6.

The second approach is a direct measurement of the output mode profile by use of the Spiricon pyroelectric array camera. The output profiles of the 500 and 2000 μm waveguides are shown in Fig. 7. The intensity distribution at the output of the 500 μm waveguide, shown in Fig. 7(a), is essentially single mode, but the intensity distribution is clearly multimode for the 2000 μm waveguide shown in Fig. 7(b). The reason that the larger bore sizes are multimode relates to the attenuation coefficient, α_{nm}, and the coupling efficiency of the power from the HE_{11} mode into the higher-order modes. From Eq. (6) we can see that $\alpha_{nm} \sim (u_{nm}\lambda)^2/a^3$, which means that for large bore sizes ($2a > \sim 500$ μm) α_{nm} is small and the higher-order modes have a lower relative loss than those for the small bore sizes ($2a < \sim 500$ μm) where α_{nm} is larger. Calculations of the ratio of the power in the HE_{nm} mode to the power in the HE_{11} mode also reveal that the mode separation increases as the bore size decreases. For example, the separation between the HE_{11} and HE_{12} modes is ~20 dB for bore sizes greater than 1000 μm, but it is more than 26 dB for the 500 μm bore size. Thus there is significantly less mode mixing in the smaller bore size waveguides.

The loss for the waveguides increases when the waveguides are bent to a radius, R. Miyagi and Kawakami[1,17] have shown that, when the waveguides are sufficiently bent, the light travels in the whispering-gallery mode; then the bending loss is $\alpha_{\text{bend}} \sim 1/R$. The bending loss also depends on the polarization of the light with respect to the plane of bending. The lowest loss occurs when E is perpendicular to the plane of bending. The bending loss measurements were made on a Plexiglas bending board with grooves corresponding to bending radii of 2.5 to 0.05 m. All these bending radii are less than the critical radius for light to travel in the whispering-gallery mode. The length of the waveguide segment under bend was kept constant at 0.31 m for all radii except the smallest radius of 0.05 m, where the bent length was 0.16 m. A linearly polarized, amplitude-stabilized CO_2 laser operating at 10.6 μm was used as the source.

The bending loss measurements for the 500 and 2000 μm bore waveguides are shown in Fig. 8. From the data, we can see the expected result that the bending loss is higher for ∥-pol compared with ⊥-pol. The slope, m, of the bending loss curves is essentially the same for all bore sizes. For ⊥-pol and ∥-pol, m is equal to 0.14 and 0.23, respectively, for the 500 μm bore. These values may be compared with the values of m equal to 0.13 and 0.20 for ⊥-pol and ∥-pol, respectively, for the 2000 μm bore guides. These values for the slope are in good agreement with those for the hollow glass waveguides at CO_2 laser wavelengths.[1]

When the waveguides are bent, some of the HE_{11} mode energy is coupled into higher-order modes. The major source of this mode coupling is surface roughness, but deformations of the circumferential geometry during bending will also lead to the generation of higher-order modes. As expected, this effect is more pronounced in the larger-bore guides. Figure 9 shows the output mode pattern for the 500 and 2000 μm bore guides when the guides are straight and then when they are bent to a radius of 0.1 m. The output remains nearly single mode for the 500 μm bore guide but clearly becomes more multimode for the bent 2000 μm bore guide.

Most of the applications envisaged for these plastic waveguides involve the transmission of incoherent light. These applications include chemical sensing and radiometry. There is also the potential for using the guides to deliver low-level laser power for laser surgery. We tested all the waveguides for CO_2 laser power transmission for power levels up to the maximum laser power of 18 W. We did not observe any measurable degradation in the transmission after 15 min at an input power of 18 W for core sizes 1000 μm and larger. The 700 μm bore guide suffered an input end meltdown after several minutes of exposure at 18 W. With the smallest 500 μm bore waveguide it was difficult to transmit greater than 5 W of power. All laser damage occurred at the input end as a result of heating of the polymer and subsequent melting of the polycarbonate. One way to circumvent this problem is to add a protective aperture at the input end of the waveguide to reflect the incident power. We have done this, using large Au-coated pinholes, but we believe that the same protection would be afforded by merely coating the end of the tube with the same Ag coating used to coat the interior surfaces. The main point is to reflect any light away from the low-melting-point polymer tubing. An alternative approach would be to undercouple light into the waveguide, but this would increase the transmission loss and lead to heating of the tubing.

Finally, we evaluated the waveguides for any effects of aging. In particular, we wanted to determine whether there were any changes in the optical properties of the guides that might result from degradation of the coatings. Our aging tests involved storing two sets of three samples each of 1500 μm bore waveguides. One set was stored for a one-year period, and the other set for three years, in the laboratory under ambient conditions. The loss values measured before and after the storage periods were essentially

unchanged. In addition, the waveguides were flexed several times, but there was no visible delamination of the coatings, and the transmission properties were unaffected. Hence, we concluded that the polycarbonate HPWs can be stored without any aging related issues' affecting the reliability of the waveguide or its transmission properties.

4. Conclusions

Polycarbonate tubing with inner Ag–AgI thin-film coatings has been shown to be an excellent waveguide for the transmission of broadband IR radiation. The losses for these polymer guides are comparable to the losses for Ag–AgI-coated hollow silica waveguides. A primary advantage of the polymer structure is that it is flexible for bore sizes considerably larger than the maximum bore size of approximately 1200 μm for silica tubing. That is, silica tubing with outer diameters of ~2000 μm or greater is rather inflexible, whereas we have made waveguides from flexible polycarbonate tubing with bore sizes as large as 6.3 mm. Therefore we expect that most applications for this technology will be for broadband sensors such as gas sensors, for which the tube is filled with the gas to be analyzed, and for use in blackbody temperature sensors. For these applications the major requirement is the preservation of as much of the input energy as possible, as source energies, such as blackbody radiation, are often small. This fact, coupled with the use of noncooled IR detectors, means that the system user will need a lowloss IR fiber. Because the loss decreases strongly ($\alpha \sim 1/a^3$) as the bore size increases, we have in the largest-bore polycarbonate waveguides the ability to achieve low loss while maintaining good flexibility.

One of the important differences between coating the polycarbonate tubing versus the silica tubing with Ag is that the polycarbonate material must first be sensitized; otherwise the Ag will not adhere well to the plastic. We developed a successful recipe for sensitization of polycarbonate tubing that led to good adhesion of the metallic films to the polymer, even after the tubing had been continually flexed. We also used the same sensitization methods on other polymers, including polyimide, PEEK brand polymer, and butyrate tubing. However, the optical properties of these other polymer waveguides were inferior to those of the polycarbonate tubing, so we abandoned the use of other polymers.

The optical loss for these polycarbonate waveguides was seen to be low, especially for the largest-bore guides fabricated. Another potential area of interest is in radiometry and chemical sensing. The loss measured for the 2000 μm bore guide at 10.6 μm was 0.02 dB/m, which, to our knowledge, is the lowest loss measured for any hollow waveguide at CO_2 laser wavelengths. Nevertheless, the measured losses are still greater than those calculated. Some reasons for this disparity may be the surface roughness of the coatings and any noncircularity, especially in bending. In addition, there is a fundamental difference in how polymer tubing is normally prepared compared with the more pristine method of glass fiber drawing used to make silica tubing. Our tubing is made by an extrusion process, which employs mold release agents and lubricants that can contaminate the inside surface. We have also observed some undulations on the surface of the extruded tubing, especially for the large core sizes. A potentially better method for fabricating the tubing would be to draw high-purity polycarbonate tubing. By employing drawing methods we would expect uniformity and surface quality that were analogous to the excellent surface quality and uniformity regularly achieved in glass fiber drawing.

References

1. J. A. Harrington, *Infrared Fiber Optics and Their Applications* (SPIE Press, 2004).
2. Y. Fink, J. N. Winn, S. Fan, C. Chen, J. Michel, J. Joannopoulos, and E. Thomas, "A dielectric omnidirectional reflector," Science **282,** 1679–1682 (1998).
3. B. Temelkuran, S. D. Hart, G. Benoit, J. D. Joannopoulos, and Y. Fink, "Wavelength-scalable hollow optical fibres with large photonic bandgaps for CO_2 laser transmission," Nature **420,** 650–653 (2002).
4. Y. Matsuura, T. Abel, and J. A. Harrington, "Optical properties of small-bore hollow glass waveguides," Appl. Opt. **34,** 6842–6847 (1995).
5. D. J. Haan and J. A. Harrington, "Hollow waveguides for gas sensing and near-IR applications," in *Specialty Fiber Optics for Medical Applications,* A. Katzir and J. A. Harrington, eds., Proc. SPIE **3596,** 43–49 (1999).
6. J. Bladon, A. Lamola, F. Lytle, W. Sonnenberg, J. Robinson, and G. Philipose, "A palladium sulfide catalyst for electrolytic plating," J. Electrochem. Soc. **143,** 1206–1213 (1996).
7. C. Rabii, D. J. Gibson, and J. A. Harrington, "Processing and characterization of silver films used to fabricate hollow glass waveguides," Appl. Opt. **38,** 4486–4493 (1999).
8. R. Dahan, J. Dror, and N. Croitoru, "Characterization of chemically formed silver iodide layers for hollow infrared guides," Mater. Res. Bull. **27,** 761–766 (1992).
9. B. Schweig, *Mirrors—A Guide to the Manufacture of Mirrors and Reflecting Surfaces* (Pelham, 1973).
10. K. Matsuura, Y. Matsuura, and J. A. Harrington, "Evaluation of gold, silver, and dielectric-coated hollow glass waveguides," Opt. Eng. **35,** 3418–3421 (1996).
11. E. D. Palik, *Handbook of Optical Constants of Solids* (Academic, 1985).
12. Y. Matsuura and J. A. Harrington, "Hollow glass waveguides with three-layer dielectric coating fabricated by chemical vapor deposition," J. Opt. Soc. Am. A **14,** 1255–1259 (1997).
13. Y. Matsuura, M. Saito, M. Miyagi, and A. Hongo, "Loss characteristics of circular hollow waveguides for incoherent infrared light," J. Opt. Soc. Am. A **6,** 423–427 (1989).
14. M. Ben David, A. Inberg, I. Gannot, and N. Croitoru, "The effect of scattering on the transmission of infrared radiation through hollow waveguides," J. Optoelectron. Adv. Mater. **1,** 23–30 (1999).
15. R. Nubling and J. A. Harrington, "Launch conditions and mode coupling in hollow glass waveguides," Opt. Eng. **37,** 2454–2458 (1998).
16. E. A. J. Marcatili and R. A. Schmeltzer, "Hollow metallic and dielectric waveguides for long distance optical transmission and lasers," Bell Syst. Tech. J. **43,** 1783–1809 (1964).
17. M. Miyagi and S. Kawakami, "Losses and phase constant changes caused by bends in the general class of hollow waveguides for the infrared," Appl. Opt. **20,** 4221–4226 (1981).